



1 **Fatty acid carbon isotopes: a new indicator of marine** 2 **Antarctic paleoproductivity?**

3 Kate Ashley¹, James Bendle¹, Xavier Crosta², Johan Etourneau^{2,3}, Philippine Campagne^{2,4},
4 Harry Gilchrist¹, Uthmaan Ibraheem¹, Sarah Greene¹, Sabine Schmidt², Yvette Eley¹,
5 Guillaume Massé^{4,5}

6 ¹School of Geography, Earth and Environmental Sciences, University of Birmingham, Edgbaston, Birmingham,
7 B15 2TT, UK

8 ²EPOC, UMR-CNRS 5805, Université de Bordeaux, 33615 Pessac, France

9 ³EPHE/PSL Research University, 75014 Paris, France

10 ⁴LOCEAN, UMR CNRS/UPCM/IRD/MNHN 7159, Université Pierre et Marie Curie, 4 Place Jussieu, 75252
11 Paris, France

12 ⁵TAKUVIK, UMI 3376 UL/CNRS, Université Laval, 1045 avenue de la Médecine, Quebec City, Quebec,
13 Canada G1V 0A6

14

15 *Correspondence to:* James Bendle (j.bendle@bham.ac.uk)

16

17 **Abstract**

18 The Antarctic coastal zone is an area of high primary productivity, particularly within coastal polynyas where
19 large phytoplankton blooms and drawdown of CO₂ occur. Reconstruction of historical primary productivity
20 changes, and the associated driving factors, could provide baseline insights on the role of these areas as sinks for
21 atmospheric CO₂, especially in the context of projected changes in coastal Antarctic sea ice. Here we investigate
22 the potential for using carbon isotopes ($\delta^{13}\text{C}$) of fatty acids in marine sediments as a proxy for primary
23 productivity. We use a highly resolved sediment core from off the coast of Adélie Land spanning the last ~400
24 years and monitor changes in the concentrations and $\delta^{13}\text{C}$ of fatty acids along with other proxy data from the
25 same core. We discuss the different possible drivers of their variability and argue that C₂₄ fatty acid $\delta^{13}\text{C}$
26 predominantly reflects phytoplankton productivity in open water environments, while C₁₈ fatty acid $\delta^{13}\text{C}$
27 reflects productivity in the marginal ice zone. These new proxies have implications for better understanding
28 carbon cycle dynamics in the Antarctica coastal zone in future paleoclimate studies.

29

30 **1 Introduction**

31 Antarctic coastal zones are important players in the global carbon cycle. The deep ocean is ventilated in these
32 regions as part of the Southern Ocean overturning circulation, allowing waters rich in nutrients and CO₂ to be
33 upwelled to the surface. In the absence of biological activity, most of the CO₂ would be leaked to the
34 atmosphere. However, coastal polynyas within the Antarctic margin are areas of very high primary productivity
35 during the spring and summer months (e.g. Arrigo et al., 2008) that rapidly reduces CO₂ to low levels through
36 photosynthesis (Arrigo and van Dijken, 2003; Arrigo et al., 2008), resulting in surface water CO₂
37 undersaturation with respect to atmospheric CO₂ (Tortell et al., 2011). The subsequent export and burial of the
38 organic carbon produced during these intense phytoplankton blooms can significantly lower atmospheric CO₂
39 concentrations (Sigman and Boyle, 2000). Therefore, any change in the consumption of these nutrients by



40 phytoplankton, or any change in phytoplankton community structure, may affect the air-sea CO₂ exchange in
41 this region.

42 Records of past phytoplankton productivity offer an opportunity to document the drivers of primary productivity
43 at different timescales from pluri-decadal to millennial. In the Antarctic coastal zone past work has focused on
44 records of organic carbon, biogenic silica and diatom abundances (Leccaroni et al., 1998; Frignani et al., 1998;
45 Denis et al., 2009; Peck et al., 2015). These proxies however may provide a biased view of phytoplankton
46 productivity as they only record a signal of siliceous productivity and may suffer from alteration during settling
47 and burial (Beucher et al., 2004; Tréguer et al., 2017). As such, there is no robust understanding of how such
48 records respond to surface water CO₂ which is of major importance in the context of Antarctic coastal sea ice
49 changes.

50 Here we investigate the use of compound specific carbon isotope analysis ($\delta^{13}\text{C}$) of algal fatty acids (FAs) in
51 marine sediments as a potential integrative proxy for reconstructing primary productivity in a polynya
52 environment. We use samples from core DTGC2011, a 4.69 m sediment core recovered from offshore Adélie
53 Land, East Antarctica, spanning the last ~400 years. The core chronology is based on radiocarbon dates and
54 confirmed by ²¹⁰Pb excess activity measurements, which indicate that DTGC2011 spans the 1580-2000 C.E.
55 period with a mean sedimentation rate of ~1 cm yr⁻¹ (Supplementary Information S1). In order to understand the
56 signal recorded by the FAs, we estimate the most likely biological source of these compounds and the habitat
57 and season of production. Moreover, we compare downcore changes in FA concentrations and $\delta^{13}\text{C}$ with other
58 proxy data from the same core.

59

60 **Environmental setting**

61 The Adélie drift is located in the Dumont D'Urville Trough in the Adélie Basin, ca. 35 km offshore from Adélie
62 Land (Fig. 1). This is a 1000 m deep, glacially scoured depression on the East Antarctic continental shelf,
63 bounded to the east by the Adélie Bank. Sea ice plays a key role on the dynamics of the region, with both fast
64 ice and pack ice present off the coast of Adélie Land. A large bank of fast ice forms annually between 135 and
65 142°E, and extends up to 120 km away from the coast (Massom et al., 2009). On the north edge of this fast ice
66 buttress is an inlet of open water forming a polynya, an area of open water surrounded by sea ice (Bindoff et al.,
67 2000).

68 The Adélie Coast is characterized by extremely high primary productivity, with phytoplankton assemblages
69 dominated by diatoms (Beans et al., 2008). The site itself is located close to the Dumont D'Urville polynya
70 (DDUP), but is also directly downwind and downcurrent of the much larger and highly productive Mertz
71 Glacier polynya (MGP) to the east (Arrigo and van Dijken, 2003).

72 The region is affected by various water masses. High Salinity Shelf Water (HSSW) is formed on the shelf in
73 coastal polynyas as a result of sea ice production and the associated brine rejection. HSSW flows out of the shelf
74 through the Adélie sill at 143°E (Fig. 1). Modified Circumpolar Deep Water (mCDW) is a warm, macronutrient-
75 rich and salty water mass which upwells onto the continental shelf through channels in the shelf break. mCDW
76 has been observed to upwell across the shelf break near the Mertz Glacier at 144°E (Williams et al., 2008) (Fig.



77 1). The Antarctic Coastal Current, also known as the East Wind Drift, flows westward often adjacent to ice
78 shelves (Thompson et al., 2018). The Antarctic Surface Water (AASW) is a widespread water mass which
79 extends across the continental shelf and has a surface mixed layer varying from a shallow (ca. 10 m), warmer
80 and fresher layer in summer to a deeper (ca. 100 m), colder layer in winter. This is also transported westward
81 along with the Antarctic Coastal Current (Martin et al., 2017). Surface waters along the Adélie coast have
82 relatively high concentrations of nitrate, silica and phosphorus, with spatially variable levels of Fe which may be
83 due to re-suspension of sediments and calving of ice (Vaillancourt et al., 2003; Sambrotto et al., 2003).

84 2 Materials and Methods

85 *Fatty acids*

86 One hundred and thirty-five sediment samples were taken for organic geochemical analyses, sampled at 1 cm
87 intervals in the top 50 cm, 2 cm intervals between 50 and 100 cm, and 5 cm intervals until 458 cm. Lipid
88 extractions were completed at the University of Birmingham using dichloromethane/methanol (3:1 v/v) and
89 ultrasonication. The acid and neutral fractions were separated using an aminopropyl-silica gel column and the
90 FAs eluted using diethyl ether with 4% acetic acid. The acid fraction was derivatized using boron trifluoride in
91 methanol and subsequently cleaned up using a silica gel column and the FAs eluted with dichloromethane. FAs
92 were identified using an Agilent gas chromatograph coupled to an Agilent mass selective detector and
93 concentrations were quantified using a gas chromatograph – flame ionization detector analysis with the
94 inclusion of an internal standard (C₁₉ alkane) of known concentration. Carbon isotopes were measured with an
95 Isoprime 100 isotope ratio-mass spectrometer coupled to an Agilent gas chromatograph-flame ionization
96 detector and a GC5 furnace. Errors are based on the standard deviation of duplicate measures and are all within
97 0.26%.

98 *HBI*s

99 Two hundred and thirty-four samples were taken every 2 cm over the whole core for highly branched
100 isoprenoids (HBI) alkenes analysis. HBI were extracted at Laboratoire d'Océanographie et du Climat:
101 Experimentations et Approches Numériques (LOCEAN), separately from the fatty acids, using a mixture of
102 9mL CH₂Cl₂/MeOH (2:1, v:v) to which internal standards were added and applying several sonication and
103 centrifugation steps in order to extract properly the selected compounds (Etourneau et al., 2013). After drying
104 with N₂ at 35°C, the total lipid extract was fractionated over a silica column into an apolar and a polar fraction
105 using 3 mL hexane and 6 mL CH₂Cl₂/MeOH (1:1, v:v), respectively. HBIs were obtained from the apolar
106 fraction by the fractionation over a silica column using hexane as eluent following the procedures reported by
107 (Belt et al., 2007, Massé et al., 2011). After removing the solvent with N₂ at 35°C, elemental sulfur was
108 removed using the TBA (Tetrabutylammonium) sulfite method (Jensen et al., 1977; Riis and Babel, 1999). The
109 obtained hydrocarbon fraction was analyzed within an Agilent 7890A gas chromatograph (GC) fitted with 30 m
110 fused silica Agilent J&C GC column (0.25 mm i.d., 0.25 µm film thickness), coupled to an Agilent 5975C
111 Series mass selective detector (MSD). Spectra were collected using the Agilent MS-Chemstation software.
112 Individual HBIs were identified on the basis of comparison between their GC retention times and mass spectra
113 with those of previously authenticated HBIs (Johns et al., 1999) using the Mass Hunter software. Values are
114 expressed as concentration relative to the internal standard.



115 *Diatoms*

116 One hundred and eighteen samples were taken every 4 cm over the whole core for diatom analyses. Sediment
117 processing and slide preparation followed the method described in Crosta et al. (2020).

118 Diatom counting followed the rules described in Crosta and Koç (2007). Around 350 diatom valves were
119 counted in each sample at a 1000X magnification on a Nikon Eclipse 80i phase contrast microscope. Diatoms
120 were identified to species or species group level. Absolute abundances of diatoms were calculated following the
121 equation detailed in Crosta et al. (2008). The relative abundance of each species was determined as the fraction
122 of diatom species against total diatom abundance in the sample.

123

124 **3 Fatty acids within DTGC2011**

125 Analysis by GC-MS identified seven dominant FAs within the DTGC2011 samples (Fig. S2). These have
126 carbon chain lengths of C₁₆ to C₂₆ and only the saturated forms (i.e. no double bonds) were identified. These are
127 predominantly even chain length FAs, with only minor amounts of the C₁₇ compound measured (Gilchrist,
128 2018).

129 **3.1 Fatty acid concentrations**

130 Down core analysis of FA concentrations reveals clear groupings in concentration changes. In the upper part of
131 the core (ca. 3 – 90 cm depth), spanning the last ~78 years, all FA compounds show a similar pattern, with
132 elevated concentrations, broadly decreasing down-core (Fig. 4). Below this, however, two groups clearly
133 diverge. These can be broadly divided into short-chained fatty acids (C₁₆ to C₂₀; SCFAs) and long-chained fatty
134 acids (C₂₂ to C₂₆; LCFAs). Within these groups, the concentrations of different compounds show similar trends,
135 but the two groups (SCFAs vs LCFAs) show different trends to each other (Gilchrist, 2018). This is confirmed
136 by R² values calculated for the linear regression of concentrations of each FA against each other throughout the
137 core (Fig. 2; n = 135, p < 0.001). Correlations between the SCFAs have R² values between 0.97 and 0.99, while
138 R² values of LCFAs range between 0.88 and 0.95. Between the two groups, however, R² values are all lower,
139 ranging between 0.50 and 0.77.

140 These distinct groupings suggest that compounds within each group (SCFAs and LCFAs) likely have a common
141 precursor organism or group of organisms, but the two groups themselves have different producers from each
142 other. These producers may in turn thrive during different seasons or within different habitats and thus, the
143 isotopic composition of compounds from these different groups may record different environmental signals.

144 R² values were also calculated for samples below 25 cm only, to remove correlations associated with
145 preservation changes in the top part of the core (discussed below). Although the R² values are not quite as high,
146 they broadly confirm these groupings, with the R² values generally being greater within the two groups (n = 73).
147 R² values range from 0.93 for the C₁₈ with C₂₀, down to 0.07 for the C₁₈ and C₂₄ (Fig. 3).

148 The C₁₈ and C₂₄ FAs are the most abundant compounds within the SCFA and LCFA groups, respectively, and
149 also the least correlated with each other both in the whole core (R² = 0.5) and below 25 cm (R² = 0.07), which
150 suggests they are the most likely to be produced by different organisms. Furthermore, these two compounds
151 yielded the highest quality isotope measurements, due to their greater concentrations, clean baseline and



152 minimal coeluting peaks (Fig. S2). Thus, these two compounds (C₁₈ and C₂₄) will be the focus of analysis and
153 discussion.

154

155 3.2 Potential sources of the C₁₈ fatty acid

156 Potential sources for the C₁₈ FA in core U1357 (recovered from the same site as DTGC2011) are discussed in
157 Ashley et al. (*in review*) who suggest the prymnesiophyte *Phaeocystis antarctica* to be the most likely main
158 producer based on a) previous studies (Dalsgaard et al., 2003), b) the high observed abundance of *P. antarctica*
159 within modern Adélie surface waters (Riaux-Gobin et al., 2011) and c) comparison between the measured δ¹³C
160 values and those reported in the literature for *P. antarctica* (Kopczynska et al., 1995; Wong and Sackett, 1978).
161 Unfortunately, the absence of *P. antarctica* in sediments, as it does not biomineralize any test, precludes the
162 direct comparison of down core trends of this species with FAs. *Phaeocystis antarctica* has been found to live
163 within and underneath sea ice before its break up, as well as in open ocean waters (Riaux-Gobin et al., 2013;
164 Poulton et al., 2007), due to its ability to use a wide range of light intensities for energy production (Moisan and
165 Mitchell, 1999).

166 Dalsgaard et al. (2003) looked at the FAs of eight major microalgal classes and showed that Prymnesiophyceae
167 and Dinophyceae produce the highest proportions of the saturated C₁₈ FA, the former to which *P. antarctica*
168 belongs. They also showed that the majority of FAs produced were the unsaturated form which are
169 preferentially broken down in the water column and sediments. As such, although the C₁₈ FA represents only a
170 small proportion of the total FA fraction, its higher preservation rate increases its proportion in the sediment.

171 Riaux-Gobin et al. (2011) found *P. antarctica* to dominate the surface waters offshore Adélie Land after spring
172 sea-ice break-up, representing 16% of the phytoplankton assemblage. Although several species of the class
173 Dinophyceae were also recorded, *P. antarctica* was more than 20 times more abundant than the 3 most abundant
174 Dinophyceae taxa combined. Sambrotto et al. (2003) also observed large blooms of *Phaeocystis* sp. in stable,
175 shallow mixed layer water along the edge of fast ice near the Mertz Glacier.

176 Furthermore, Skerratt et al. (1998) identified the FAs produced by *P. antarctica* and two Antarctic diatoms,
177 *Chaetoceros simplex* and *Odontella weissflogii*, from culture samples. Of the FAs produced by *P. antarctica*,
178 52% were saturated FAs (C₁₄-C₂₀) compared to just 14 and 11% for the two diatoms, respectively, the latter
179 instead producing much more of the mono- and polyunsaturated FAs. The percentage of C₁₈ FA produced by *P.*
180 *antarctica* was also 4.1 and 12.5 times greater than the percentage of C₁₈ produced by *C. simplex* and *O.*
181 *weissflogii*, respectively. This supports the hypothesis of *P. antarctica* being a dominant and abundant source of
182 the saturated C₁₈ FA in the Adélie basin though minor contributions of C₁₈ from other phytoplankton species
183 such as the diatoms and dinoflagellates cannot be excluded.

184 3.3 Potential sources of the C₂₄ fatty acid

185 Long-chain *n*-alkyl compounds, including FAs, are major components of vascular plant waxes and their
186 presence within sediments has commonly been used as a biomarker of terrestrial plants (Pancost and Boot,
187 2004). Although plants such as bryophytes (e.g. mosses) which are present in the Antarctic do also produce
188 LCFAs (Salminen et al., 2018), it is unlikely that FAs from terrestrial plants make a significant contribution to



189 the water column, due to their extremely limited extent on the continent, and the significant distance of the site
190 from other continental sources.

191 However, there is much evidence in the literature for various aquatic sources of LCFAs, a few of which are
192 summarized in Table S2. Although not all of these sources are likely to be present within the coastal waters
193 offshore Adélie Land, it highlights the wide range of organisms which can produce these compounds, and thus
194 suggests that an autochthonous marine source is entirely possible, especially considering the highly productive
195 nature of this region.

196 **3.4 Microbial degradation and diagenetic effects on fatty acid concentration**

197 Both the C₁₈ and C₂₄ FAs show an overall decrease in concentrations down-core, with significantly higher
198 concentrations in the top 80 cm (representing ~70 years) compared to the rest of the core. Below this point, FAs
199 concentrations variations are attenuated (Fig. 4).

200 Many studies have shown that significant degradation of FAs occurs both within the water column and surface
201 sediments as a result of microbial activity, and that there is preferential break down of both short-chained and
202 unsaturated FA, compared to longer-chained and saturated FA (Haddad et al., 1992; Matsuda, 1978; Colombo et
203 al., 1997). Haddad et al. (1992) studied the fate of FAs within rapidly accumulating (10.3 cm yr⁻¹) coastal
204 marine sediments (off the coast of North Carolina, USA) and showed that the vast majority (ca. 90%) of
205 saturated FAs were lost due to degradation within the top 100 cm (representing ~10 years). Similarly, Matsuda
206 and Koyama (1977) found FA concentrations decrease rapidly within the top 20 cm of sediment (accumulating
207 at 4 mm yr⁻¹) from Lake Suwa, Japan. Assuming similar processes apply to the DTGC2011 sediments, this
208 suggests the declining concentrations within the upper part of the core are largely the result of diagenetic effects
209 such as microbial activity occurring within the surface sediments, and thus do not reflect a real change in
210 production of these compounds in the surface waters.

211 The complete lack of both unsaturated and short chained (fewer than 16 carbon atoms) FA compounds
212 identified within DTGC2011 samples, even within the top layers, suggests that selective breakdown of
213 compounds has already occurred within the water column and on the sea floor (before burial). Wakeham et al.
214 (1984) assessed the loss of FAs with distance during their transport through the water column at a site in the
215 equatorial Atlantic Ocean and estimated that only 0.4 to 2% of total FAs produced in the euphotic zone reached
216 a depth of 389 m, and even less reaching more than 1,000 m depth, the vast majority of material being recycled
217 in the upper water column. Their results also show a significant preference for degradation of both unsaturated
218 and short chained compounds over saturated and longer chain length compounds. Although no studies into the
219 fate of lipids within the water column exist for the Adélie region, the >1,000 m water depth at the core site
220 would provide significant opportunity for these compounds to be broken down during transportation through the
221 water column. It is likely, therefore, that the distribution of compounds preserved within the sediments will not
222 be a direct reflection of production in the surface waters, and explains the preference for saturated FAs with
223 carbon chain lengths of 16 and more.

224 Although FA concentrations in the top 80 cm of core DTGC2011 are much higher overall than the sediments
225 below and show a broad decline over this section, there is a high level of variability. Concentrations do not
226 decrease uniformly within the top part of the core, as may be expected if concentration change is a first order



227 response to declining microbial activity. The peak in total FAs instead occurs at a depth of 21-22 cm with a
228 concentration more than an order of magnitude higher than in the top layer. This variability creates difficulty in
229 directly determining the effects of diagenesis. However, by 25 cm the concentrations drop to below 1,000 ng g⁻¹
230 and remain so until 32 cm before increasing again. This may suggest that diagenetic effects of FA
231 concentrations are largely complete by 25 cm (representing ca. 25 years), consistent with results from Haddad et
232 al. (1992) and Matsuda and Koyama (1977), and that subsequent down-core concentration variations
233 predominantly represent real changes in export productivity, resulting from environmental factors. However, the
234 fluctuating nature of concentrations particularly in the youngest sediments means it is difficult to clearly unpick
235 the effects of diagenesis from actual changes in production of these compounds, and a clear cut-off point for
236 diagenetic effects cannot be determined.

237 3.5 Comparison of fatty acid concentrations with highly branched isoprenoid alkenes

238 We compare FA concentrations with other organic compounds (whose source is better constrained) in
239 DTGC2011 to better understand FA sources. Direct comparison between different organic compound classes
240 can be made since both are susceptible to similar processes of diagenesis, in contrast to other proxies such as
241 diatoms. In core DTGC2011, concentrations of di- and tri-unsaturated highly branched isoprenoid (HBI) alkenes
242 (referred to as HBI diene and HBI triene, respectively hereafter) were available.

243 In Antarctic marine sediments HBIs have been used as a tool for reconstructing sea ice (Belt et al., 2016, 2017).
244 Smik et al. (2016) compared the concentrations of HBIs in sediment samples offshore East Antarctica from the
245 permanently open-ocean zone (POOZ), the marginal ice zone (MIZ) and the summer sea-ice zone (SIZ). They
246 found the HBI diene reached the highest concentrations in the SIZ and was absent from the POOZ. In contrast,
247 the HBI triene was most abundant in the MIZ, i.e. at the retreating sea ice edge, with much lower concentrations
248 in the SIZ and POOZ. This suggests that the two compounds are produced in contrasting environments but
249 remain sensitive to changes in sea ice.

250 The HBI diene biomarker (or IPSO₂₅ for Ice Proxy Southern Ocean with 25 Carbons) is mainly biosynthesised
251 by *Berkeleya adeliensis* (Belt et al., 2016), a diatom which resides and blooms within the sea ice matrix, and
252 thus can be used as a proxy for fast ice attached to the coast. In contrast, the presence of the HBI triene mostly in
253 the MIZ is suggestive of a predominantly pelagic phytoplankton source (e.g. *Rhizosolenia* spp, Massé et al.,
254 2011; Smik et al., 2016; Belt et al., 2017), rather than sea-ice dwelling diatoms (Smik et al., 2016). The fact that
255 HBI triene reached its greatest abundance within the MIZ suggests its precursor organism may thrive in the
256 stratified, nutrient-rich surface waters of the sea-ice edge.

257 One key similarity between both the HBI diene and triene, and the FA concentrations is that the highest
258 concentrations are found in the youngest sediments. These compounds all show broad increases in concentration
259 from 110 cm depth (ca. 1900 C.E) until the top of the core (Fig. 4 and 5). Concentrations of HBIs are also
260 susceptible to degradation through the water column through visible light induced photo-degradation (Belt and
261 Müller, 2013) and diagenetic effects, as well as reacting with sediments resulting in sulphurisation (Sinninghe
262 Damsté et al., 2007), isomerisation and cyclisation (Belt et al., 2000). Thus, it is likely that the elevated
263 concentrations, and thus the similarity between FA and HBI concentrations, is due to better preservation at the
264 top of the core, with diagenetic effects having an increasing and progressive impact down to ca. 25cm depth.



265 However, despite an overall increase in HBI and FA concentrations above 110 cm depth, there are clear
266 deviations from this trend. Concentrations of the HBI triene show some broad similarities with FA
267 concentrations. In particular, both the HBI triene and the C₁₈ FA have coeval concentration peaks around 1980-
268 88, 1967, 1938, 1961-72, 1848 and 1752 C.E. (Fig. 5). These peaks are offset from the HBI diene
269 concentrations, suggesting that they result from increased production in the surface waters rather than simply
270 changes in preservation. The HBI triene is more susceptible to degradation than the diene (Cabedo Sanz et al.,
271 2016), so while this could explain some of the differences between the diene and triene records, where the triene
272 increases independently of the diene, this is likely to be a genuine reflection of increased production of these
273 compounds at the surface rather than an artefact of preservation processes.

274 This close similarity between the C₁₈ FA and HBI triene concentrations (Fig. 5) suggests that the C₁₈ may also
275 be produced by an organism associated with the retreating ice edge. *Phaeocystis antarctica* has been proposed
276 as a potential producer of the C₁₈ in core U1357B (Ashley et al., *in review*). In the Ross Sea, *P. antarctica* has
277 been observed to dominate the phytoplankton bloom during the spring, blooming in deep mixed layers as the sea
278 ice begins to melt, after which diatoms tend to dominate during the summer (Arrigo et al., 1999; Tortell et al.,
279 2011; DiTullio et al., 2000). However, a few studies in the Adélie region suggest this is not the case there.
280 Offshore Adélie Land, *P. antarctica* has been found to only appear late in the spring/early summer, later than
281 many diatom species. During this time, it occurs preferentially within the platelet ice and under-ice water
282 (Riaux-Gobin et al., 2013). Furthermore, Sambrotto et al. (2003) observed a surface bloom of *P. antarctica* near
283 the Mertz Glacier (Fig. 1) during the summer months, in very stable waters along the margin of fast ice and
284 Riaux-Gobin et al. (2011) found *P. antarctica* to be abundant in the coastal surface waters eight days after ice
285 break up. This indicates an ecological niche relationship with cold waters and ice melting conditions. This might
286 explain the close similarity between the C₁₈ and HBI triene concentrations, both produced by organisms
287 occupying a similar habitat at the ice edge.

288 The C₂₄ FA record also shows some similarity with the HBI triene record. This appears to be mostly in the top
289 part of the core where the highest concentrations are found. The reason for this resemblance is unclear,
290 especially considering the lack of correlation between the C₂₄ and C₁₈ FA concentrations. However, it may relate
291 to the better preservation in younger samples. The weaker coherence between the C₂₄ and the HBI triene, and
292 also HBI diene, suggests that the C₂₄ FA is predominantly produced by an organism which is not associated with
293 sea ice, and thus instead with more open waters.

294 Seventy-three diatom species were encountered in core DTGC2011 (Campagne, 2015), with *Fragilariopsis*
295 *curta* and *Chaetoceros* resting spores being the most abundant. However, trends in diatom abundances do not
296 show any clear correlations with the C₁₈ or C₂₄ FA concentrations. While this would lend support to the
297 hypothesis that diatoms are not the main producers of these compounds, the differing effects of diagenesis on
298 the preservation of diatoms and lipids could also explain some of the differences in observed concentrations,
299 particularly in the upper part of the core. The known producer of the HBI diene, *Berkeleya adeliensis*, for
300 example, was not recorded within the core, likely due to their lightly silicified frustules which are more
301 susceptible to dissolution (Belt et al., 2016). Therefore, despite the lack of a correlation between diatom
302 abundances and FA concentrations, we cannot entirely rule out the possibility of a minor contribution of FAs by
303 diatoms.



304 **4 Carbon isotopes of fatty acids**

305 Down-core changes in $\delta^{13}\text{C}$ for the C_{18} and C_{24} FAs ($\delta^{13}\text{C}_{18\text{FA}}$ and $\delta^{13}\text{C}_{24\text{FA}}$, respectively) (Fig. 6 and 7) clearly
306 show different trends, with very little similarity between them ($R^2 = 0.016$). This further supports the idea that
307 these compounds are being produced by different organisms, and thus are recording different information.

308 The mean carbon isotope value of $\delta^{13}\text{C}_{18\text{FA}}$ of -29.8‰ in core U1357 from the same site (Ashley et al., *in*
309 *review*) is suggestive of a pelagic phytoplankton source (Budge et al., 2008). In core DTGC2011 the mean
310 values of $\delta^{13}\text{C}_{18\text{FA}}$ and $\delta^{13}\text{C}_{24\text{FA}}$ are -26.2‰ and -27.6‰ , respectively. Though more positive, these values are
311 still within the range of a phytoplankton source. Additionally, the 0.5‰ more positive $\delta^{13}\text{C}_{18\text{FA}}$ mean value over
312 the $\delta^{13}\text{C}_{24\text{FA}}$ may indicate the contribution of sea-ice dwelling algae producers, since carbon fixation occurring
313 within the semi-closed system of the sea ice will lead to a higher degree of CO_2 utilisation than in surrounded
314 open waters (Henley et al., 2012). Although no studies on FA $\delta^{13}\text{C}$ of different organisms are available for the
315 Southern Ocean, Budge et al. (2008) measured the mean $\delta^{13}\text{C}$ value of C_{16} FA from Arctic sea-ice algae (-24.0
316 ‰) to be 6.7‰ higher than pelagic phytoplankton (-30.7‰) from the same region.

317 The higher $\delta^{13}\text{C}$ of the C_{18} FA could therefore be indicative of *P. antarctica* living partly within the sea ice, e.g.
318 during early spring before ice break up. The more negative $\delta^{13}\text{C}_{24\text{FA}}$ suggests it is more likely to be produced by
319 phytoplankton predominantly within open water.

320 **4.1 Controls on $\delta^{13}\text{C}_{\text{FA}}$**

321 The $\delta^{13}\text{C}_{18\text{FA}}$ record shows a broadly increasing trend towards more positive values from ca. 1587 until ca. 1920
322 C.E., with short term fluctuations of up to $\sim 4\text{‰}$ superimposed on this long-term trend (Fig. 7). This is followed
323 by a period of higher variability with a full range of 5.6‰ until the most recent material (ca. 1999 C.E.), with
324 more negative $\delta^{13}\text{C}$ values between 1921 and 1977 C.E. and rapid a shift toward more positive values thereafter.
325 In contrast, the $\delta^{13}\text{C}_{24\text{FA}}$ record overall shows a weak, negative trend, with large decadal fluctuations of up to 4.6
326 ‰ , with a more pronounced negative trend after ca. 1880 C.E. (Fig. 6 and 7).

327 Below we consider the various factors which may control the carbon isotope value of algal biomarkers produced
328 in the surface waters. Down-core changes in FA $\delta^{13}\text{C}$ are likely to be a function of either the $\delta^{13}\text{C}$ of the
329 dissolved inorganic carbon (DIC) source, changes in the species producing the biomarkers, diagenesis or
330 changing photosynthetic fractionation (ϵ_p). The next section outlines the potential influence of these factors may
331 have in order to assess the mostly likely dominant driver of FA $\delta^{13}\text{C}$.

332 *4.1.1 Isotopic composition of DIC*

333 The $\delta^{13}\text{C}$ of the DIC source can be affected by upwelling or advection of different water masses, or the $\delta^{13}\text{C}$ of
334 atmospheric CO_2 . Around the Antarctic, distinct water masses have unique carbon, hydrogen and oxygen
335 isotope signatures and thus isotopes can be used as water mass tracers (e.g. Mackensen, 2001, Archambeau et
336 al., 1998). In the Weddell Sea for example, Mackensen (2001) determined the $\delta^{13}\text{C}$ value of eight water masses,
337 which ranged from 0.41‰ for Weddell Deep Water, sourced from CDW, to 1.63‰ for AASW. A similar
338 range of $\sim 1.5\text{‰}$ was identified in water masses between the surface and $\sim 5,500$ m depth along a transect from
339 South Africa to the Antarctic coast (Archambeau et al., 1998). Assuming similar values apply to these water
340 masses offshore Adélie Land, this range in values would be insufficient to explain the $\sim 5\text{‰}$ variation of $\delta^{13}\text{C}$



341 recorded by both C_{18} and C_{24} FA, even in the situation of a complete change in water mass over the core site.
342 Furthermore, site DTGC2011, located within a 1,000 m deep depression and bounded by the Adélie Bank to the
343 north, is relatively sheltered from direct upwelling of deep water (Fig. 1). Though inflow of mCDW has been
344 shown to occur within the Adélie Depression to the east of the bank (Williams and Bindoff, 2003) and possibly
345 within the Dumont d'Urville Trough, only very small amplitude changes in $\delta^{13}C$ of benthic foraminifera,
346 tracking upper CDW, have been observed over the Holocene in Palmer Deep, West Antarctica (Shevenell and
347 Kennett, 2002). Although from a different location, this argues against large changes in the isotopic composition
348 of the source of mCDW.

349 Changes in the $\delta^{13}C$ of atmospheric CO_2 , which is in exchange with the surface waters could also have the
350 potential to drive changes in the $\delta^{13}C$ of algal biomarkers. Over the last ca. 200 years, the anthropogenic burning
351 of fossil fuels has released a large amount of CO_2 depleted in ^{13}C , meaning that the $\delta^{13}C$ of CO_2 has
352 decreased by ca. 1.5 ‰, as recorded in the Law Dome ice core. Prior to this, however, the $\delta^{13}C$ of CO_2 in the
353 atmosphere remained relatively stable, at least for the last thousand years (Francey et al., 1999). Therefore, this
354 could potentially drive the $\delta^{13}C$ of algal biomarkers towards lighter values within the last 200 years, but this
355 could not explain the full variation of ~5-6 ‰ in FA $\delta^{13}C$ measured throughout the core. No clear trend towards
356 lighter values is evident in the last 200 years of the FA $\delta^{13}C$ records, which suggests that this change is
357 insignificant compared to local and regional inter-annual variations as a result of other environmental drivers
358 (discussed below).

359 4.1.2 Changing species

360 A shift in the organisms producing the FA could also affect $\delta^{13}C$ where species have different fractionation
361 factors. For example, changing diatom species have been shown to have an effect on bulk organic matter $\delta^{13}C$ in
362 core MD03-2601, offshore Adélie Land, over the last 5 ka (Crosta et al., 2005). However, the bulk organic
363 matter might have contained other phytoplankton groups than diatoms with drastically different $\delta^{13}C$ values and
364 fractionation factors. Here we measured $\delta^{13}C$ of individual biomarkers, produced by a more restricted group of
365 phytoplankton groups (possibly restricted to a few dominant species) compared to bulk $\delta^{13}C$. As discussed
366 above, the C_{18} appears to be produced predominantly by *P. antarctica*, whereas diatoms do not tend to produce
367 this compound (Dalsgaard et al., 2003).

368 4.1.3 Effect of diagenesis on lipid $\delta^{13}C$

369 Sun et al. (2004) studied the carbon isotope composition of FAs during 100 days of incubation in both oxic and
370 anoxic seawater. They observed a shift towards more positive values in FA $\delta^{13}C$, ranging between 2.6 ‰ for the
371 $C_{14:0}$ and as much as 6.9‰ in the $C_{18:1}$, under anoxic conditions. This suggests that diagenesis could affect FA
372 $\delta^{13}C$ in core DTGC2011. However, these observed changes are rapid (days to months), occurring on timescales
373 which are unresolvable in the FA $\delta^{13}C$ record (annual to decadal), and thus may have no effect on the trends
374 observed in our record. Based on concentration data discussed above, it seems that diagenetic overprint is
375 largely complete by ~25 cm (Fig. 4). In the top 25 cm of the core, the $\delta^{13}C_{24FA}$ values increase by ~2.5 ‰,
376 downward ($R^2 = 0.63$, $n = 11$) while the $\delta^{13}C_{18FA}$ values display a large variation with no overall trend ($R^2 =$
377 0.12, $n = 20$). If diagenesis was driving the changes in $\delta^{13}C$, it is likely that this trend would be observed in all
378 FA compounds.



379 Taken together, it appears that neither changes in the $\delta^{13}\text{C}$ of the DIC, changing phytoplankton groups nor
380 diagenesis can fully explain the variation of FA $\delta^{13}\text{C}$ recorded within DTGC2011. Therefore, we hypothesise
381 that changes in ϵ_p are the main driver of FA $\delta^{13}\text{C}$.

382 **4.2 Controls on photosynthetic fractionation (ϵ_p)**

383 There is a positive relationship between ϵ_p in marine algae and dissolved surface water $\text{CO}_{2(\text{aq})}$ concentration
384 (Rau et al., 1989). As a result, higher $\delta^{13}\text{C}$ values are hypothesised to reflect lower surface water $\text{CO}_{2(\text{aq})}$ and vice
385 versa. Changes in surface water $\text{CO}_{2(\text{aq})}$ concentration in turn may be driven by various factors, including
386 changing atmospheric CO_2 (Fischer et al., 1997), wind-driven upwelling of deep, carbon-rich water masses
387 (Sigman and Boyle, 2000; Takahashi et al., 2009), sea-ice cover (Henley et al., 2012) and/or primary
388 productivity (Villinski et al., 2008). Thus, determining the main driver(s) of surface water CO_2 changes offshore
389 Adélie Land should enable interpretation of the DTGC2011 FA $\delta^{13}\text{C}$ records.

390 *4.2.1 Sea ice*

391 Brine channels within sea ice have very low CO_2 concentrations and a limited inflow of seawater. Carbon
392 isotopic fractionation of algae living within these channels has been shown to be greatly reduced compared to
393 organisms living in the surrounding open waters (Gibson et al., 1999), leading to elevated $\delta^{13}\text{C}$ values. It is thus
394 possible that, under conditions of high sea-ice cover, enhanced FA contribution from sea-ice algae leads to
395 elevated sedimentary $\delta^{13}\text{C}$ values. HBI diene concentrations within DTGC2011 show a much greater presence
396 of fast ice at the core site ca. 1960 C.E (Fig. 5). However, during this time there is no clear elevation in $\delta^{13}\text{C}$
397 concentrations in either $\delta^{13}\text{C}_{18\text{FA}}$ or $\delta^{13}\text{C}_{24\text{FA}}$, both instead showing generally lower $\delta^{13}\text{C}$ values. In fact, $\delta^{13}\text{C}_{18\text{FA}}$
398 shows the lowest values of the whole record between 1925 and 1974 C.E., during which sea ice, as recorded by
399 the HBI diene, is at its highest level. This suggests that inputs in sea-ice algae at this time are not driving
400 changes in FA $\delta^{13}\text{C}$.

401 The DTGC2011 core site sits proximal to the Dumont D'Urville polynya, which has a summer area of $13.02 \times$
402 10^3 km^2 and a winter area of $0.96 \times 10^3 \text{ km}^2$ (Arrigo and van Dijken, 2003). Changes in the size of the polynya
403 both on seasonal and inter-annual time scales will affect air-sea CO_2 exchange and thus also surface water CO_2
404 concentration. A reduced polynya may lead to greater supersaturation of CO_2 in the surface waters due to
405 reduced outgassing, allowing CO_2 to build up below the ice, leading to lower $\delta^{13}\text{C}$ values of algal biomarkers
406 produced in that habitat (Massé et al., 2011). Thus changes in the extent of sea ice may also effect FA $\delta^{13}\text{C}$.

407 *4.2.2 Observed trends in surface water $\text{CO}_{2(\text{aq})}$*

408 If the trend in surface water $\text{CO}_{2(\text{aq})}$ paralleled atmospheric CO_2 , with an increase of over 100 ppm over the last
409 200 years (MacFarling Meure et al., 2006), we might expect phytoplankton to exert a greater fractionation
410 during photosynthesis in response to elevated surface water $\text{CO}_{2(\text{aq})}$ concentration, resulting in more negative
411 $\delta^{13}\text{C}$ values. Taking into account the decline in atmospheric $\delta^{13}\text{C}_{\text{CO}_2}$ over the same period would further enhance
412 the reduction in phytoplankton $\delta^{13}\text{C}$. Fischer et al. (1997) looked at the $\delta^{13}\text{C}$ of both sinking matter and surface
413 sediments in the South Atlantic and suggested that, since the preindustrial, surface water $\text{CO}_{2(\text{aq})}$ has increased
414 much more in the Southern Ocean than in the tropics. They estimated that a 70 ppm increase in $\text{CO}_{2(\text{aq})}$ in
415 surface waters of 1°C would decrease phytoplankton $\delta^{13}\text{C}_{\text{org}}$ by ca. 2.7‰, and up to 3.3‰ $\delta^{13}\text{C}_{\text{CO}_2}$ change are
416 included, between preindustrial and 1977-1990. However, sea ice cover and summer primary productivity are



417 likely to be much higher off Adélie Land than in the South Atlantic, both of which will affect air-sea gas
418 exchange.

419 Shadwick et al. (2014) suggest that surface water CO₂ should track the atmosphere in the Mertz Polynya region,
420 despite the seasonal ice cover limiting the time for establishing equilibrium with the atmosphere. They
421 calculated wintertime CO₂ in the shelf waters of the Mertz Polynya region, offshore Adélie Land (Fig. 1),
422 measuring ca. 360 ppm in 1996, ca. 396 ppm in 1999, and ca. 385 ppm in 2007, while atmospheric CO₂ at the
423 South Pole was 360, 366 and 380 ppm, respectively (Keeling et al., 2005). Based on the 1996 and 2007 data
424 only, an increase in CO₂ of ca. 25 ppm is observed over these 11 years, coincident with the 20 ppm atmospheric
425 CO₂ increase over this time period. However, high interannual variability (\pm ca. 30 ppm) is evident (e.g. 396
426 ppm in 1999) suggesting that other factors, particularly upwelling, may override this trend. The latter was also
427 suggested by Roden et al. (2013) based on winter surface water measurements in Prydz Bay, indicating that
428 decadal-scale carbon cycle variability is nearly twice as large as the anthropogenic CO₂ trend alone.

429 During the austral winter, upwelling of deep water masses causes CO₂ to build up in the surface waters, and sea
430 ice cover limits gas exchange with the atmosphere (Arrigo et al., 2008; Shadwick et al., 2014). Although only
431 limited data, the measurements by Shadwick et al. (2014) suggest slight supersaturation, of up to 30 ppm, occurs
432 in the winter due to mixing with carbon-rich subsurface water, but with high interannual variability. This is
433 compared to undersaturation of 15 to 40 ppm during the summer as a result of biological drawdown of CO₂.
434 Roden et al. (2013) also observed varying levels of winter supersaturation in Prydz Bay, East Antarctica, with
435 late winter CO₂ values of 433 ppm in 2011 (45 μ atm higher than atmospheric CO₂), and suggested that
436 intrusions of C-rich mCDW onto the shelf may play a part in this. Similarly, winter surface water CO₂ of 425
437 ppm has been measured by Sweeney (2003) in the Ross Sea, before being drawn down to below 150 ppm in the
438 summer as phytoplankton blooms develop.

439 Enhanced upwelling of deep carbon-rich waters in the Southern Ocean are thought to have played a key role in
440 the deglacial rise of atmospheric CO₂, increasing CO₂ concentrations by ~80 ppm (Anderson et al., 2009; Burke
441 and Robinson, 2012). Changes in upwelling offshore Adélie Land could therefore drive some interannual
442 variability in surface water CO₂ and hence FA $\delta^{13}\text{C}$ in DTGC2011. However, upwelling tends to be stronger
443 during the winter months, when sea-ice formation and subsequent brine rejection drive mixing with deeper C-
444 rich waters. At this time, heavy sea-ice cover limits air-sea gas exchange and enhances CO₂ supersaturation in
445 regional surface waters (Shadwick et al., 2014). In contrast, the phytoplankton producing FA thrive during the
446 spring and summer months during which CO₂ is rapidly drawn down and the surface waters become
447 undersaturated. However, upwelling cannot be discarded as a possible contributor to surface water CO₂ change.
448 However, the core site is in a relatively sheltered area and is probably not affected by significant upwelling.

449 Based on these studies, changes in atmospheric CO₂ concentration and $\delta^{13}\text{C}$ of the source appear to be unlikely
450 to be a dominant driver of the FA $\delta^{13}\text{C}$ record, with interannual variations driven by other factors overriding any
451 longer-term trend. There is also no clear anthropogenic decline in the FA $\delta^{13}\text{C}$ record over the last 200 years,
452 which supports this hypothesis.

453 *4.2.3 Productivity*



454 Given that changes in atmospheric CO₂, source signal, sea ice algae or diagenesis seem unable to explain the
455 full range of variability seen in the FA δ¹³C record, the most plausible driver appears to be changes in surface
456 water primary productivity. Coastal polynya environments in the Antarctic are areas of very high primary
457 productivity (Arrigo and van Dijken, 2003). The DTGC2011 core site sits near to the Dumont D'Urville
458 polynya, and is just downstream of the larger and more productive MGP (Arrigo and van Dijken, 2003). In large
459 polynyas such as the Ross Sea, primary productivity leads to intense drawdown of CO₂ in the surface waters,
460 resulting in reduced fractionation by the phytoplankton during photosynthesis (Villinski et al., 2008). In the
461 Ross Sea, surface water CO₂ has been observed to drop to below 100 ppm during times of large phytoplankton
462 blooms (Tortell et al., 2011) demonstrating that primary productivity can play a key role in controlling surface
463 water CO₂ concentrations in a productive polynya environment. Arrigo et al. (2015) found the MGP to be the 8th
464 most productive polynya in the Antarctic (out of 46) based on total net primary productivity during their
465 sampling period, and Shadwick et al. (2014) observed CO₂ drawdown in the MGP during the summer months.

466 Therefore, we suggest that FA δ¹³C signals recorded in DTGC2011 is predominantly a signal of surface water
467 CO₂ driven by primary productivity. Indeed, the potential for the δ¹³C of sedimentary lipids to track surface
468 water primary productivity has been recognised in the highly productive Ross Sea polynya. High variability in
469 surface water CO₂ values have been measured across the polynya during the summer months (December –
470 January), ranging from less than 150 ppm in the western Ross Sea near the coast, to >400 ppm on the northern
471 edge of the polynya. This pattern was closely correlated with diatom abundances, indicating intense drawdown
472 of CO₂ in the western region where diatom abundances were highest (Tortell et al., 2011). This spatial variation
473 in productivity is recorded in particulate organic carbon (POC) δ¹³C, and is also tracked in the surface sediments
474 by total organic carbon (TOC) δ¹³C and algal sterol δ¹³C, all of which show significantly higher values in the
475 western Ross Sea. This spatial pattern in sterol δ¹³C was concluded to be directly related to CO₂ drawdown at
476 the surface, resulting in average sterol δ¹³C values varying from -27.9‰ in the west, where productivity is
477 greatest, down to -33.5‰ further offshore (Villinski et al., 2008).

478 A similar relationship is evident in Prydz Bay, where POC δ¹³C was found to be positively correlated with POC
479 concentration and negatively correlated with nutrient concentration, indicating greater drawdown of CO₂ and
480 nutrients under high productivity levels (Zhang et al., 2014).

481 This suggests it is possible to apply FA δ¹³C as a palaeoproductivity indicator in the highly productive Adélie
482 polynya environment. However, it is important to constrain the most likely season and habitat being represented,
483 since phytoplankton assemblages vary both spatially (e.g. ice edge or open water) and temporally (e.g. spring or
484 summer). The incredibly high sedimentation rate (1-2 cm yr⁻¹) within the Adélie Basin is thought to result, on
485 top of regional high productivity, from syndepositional focusing processes bringing biogenic debris from the
486 shallower Adélie and Mertz banks to the ca. 1,000 m deep basin (Escutia et al., 2011). Thus, it is likely that core
487 DTGC2011 contains material from a wide area, including both the Mertz and Dumont d'Urville polynyas, and
488 areas both near the coast and further offshore, meaning it is quite possible that the C₁₈ and C₂₄ FAs are
489 integrating palaeoproductivity changes weighted towards different regional environments, which would explain
490 their different trends. Furthermore, surface water CO₂ can vary spatially, such as in the Ross Sea polynya where
491 Tortell et al. (2011) measured surface water CO₂ values ranging between 100 and 400 ppm. Thus, it is likely



492 that these two areas offshore Adélie Land where the C₁₈ and C₂₄ FAs are being produced will also have differing
493 surface water CO₂ concentrations and trends.

494 4.3 Comparison of fatty acid δ¹³C with other proxy data

495 Comparison of down-core variations in FA δ¹³C with other proxy data can also be used to decipher the main
496 signal recorded. Comparison between δ¹³C_{24FA} and the major diatom species abundances within the core shows
497 a reasonably close coherence with *Fragilariopsis kerguelensis*, particularly since ~1800 C.E. (Fig. 6).
498 *Fragilariopsis kerguelensis* is an open water diatom species and one of the most dominant phytoplankton
499 species offshore Adélie Land (Chiba et al., 2000), reaching its peak abundance in the summer (Crosta et al.,
500 2007). This suggests that the C₂₄ FA is being produced during the summer months and, as such, is reflecting
501 productivity in more open waters. The δ¹³C_{24FA} record does not show any similarity to the sea-ice records, as
502 inferred by HBI diene concentrations and abundances of *Fragilariopsis curta* (Fig. 6 and 7), here again
503 suggesting that these compounds are being produced in open water during the summer months after sea ice has
504 retreated.

505 As discussed above, *P. antarctica* is a likely producer for the C₁₈ FA, a prymnesiophyte algae which has been
506 observed in the Adélie region in summer months residing predominantly along the margin of fast ice, but also
507 further offshore (Riaux-Gobin et al., 2013, 2011; Vaillancourt et al., 2003). The aversion of *F. kerguelensis* to
508 sea ice (and thus also the C₂₄ FA producer) in contrast to *P. antarctica*, may explain the clear lack of coherence
509 in the down-core trends in δ¹³C_{18FA} and δ¹³C_{24FA} (Fig. 7). Thus, we hypothesise that δ¹³C_{18FA} is recording surface
510 water CO₂ driven by productivity in the MIZ, whilst δ¹³C_{24FA} is recording surface water CO₂ in more open
511 water, further from the sea-ice edge.

512 HBI diene concentrations indicate elevated fast ice cover between ~1919 and 1970 C.E., with a particular peak
513 between 1942 and 1970 C.E., after which concentrations rapidly decline and remain low until the top of the core
514 (Fig. 7). Abundances of *F. curta*, used as a sea-ice proxy, similarly show peaks at this time indicate increased
515 sea-ice concentration (Campagne, 2015) (Fig. 7). δ¹³C_{18FA} indicates a period of low productivity between ~1922
516 and 1977 C.E., broadly overlapping with this period of elevated fast ice concentration (Fig. 7), with a mean
517 value of -27.12‰. This is compared to the mean value of -26.23‰ in the subsequent period (~1978 to 1998
518 C.E.) during which HBI diene concentration remain low (Fig. 7). This suggests that productivity in the coastal
519 region was reduced, while sea-ice concentrations were high. This might be expected during a period of
520 enhanced ice cover – perhaps representing a reduction in the amount of open water, or a shorter open water
521 season – since the majority of productivity generally takes place within open water (Wilson et al., 1986).

522 Furthermore, δ¹³C_{18FA} shows a broad similarity with *Chaetoceros* resting spores (CRS) on a centennial scale,
523 with lower productivity at the start of the record, ca. 1587 to 1662 C.E., followed by an increase in both proxies
524 in the middle part of the record, where δ¹³C_{18FA} becomes relatively stable and CRS reaches its highest
525 abundances of the record. This is then followed in the latter part of the record, after ca. 1900 C.E., by both
526 proxies displaying lower values overall. CRS are associated with high nutrient levels and surface water
527 stratification along the edge of receding sea ice, often following high productivity events (Crosta et al., 2008).
528 The broad similarity to CRS, with lower values recorded during periods of high sea-ice concentrations, suggests



529 that $\delta^{13}\text{C}_{18\text{FA}}$ is similarly responding to productivity in stratified water at the ice edge. This supports the
530 hypothesis that $\delta^{13}\text{C}_{18\text{FA}}$ is recording primary productivity in the MIZ.

531 5 Conclusions

532 FAs identified within core DTGC2011, recovered from offshore Adélie Land, were analysed for their
533 concentrations and carbon isotope compositions to assess their utility as a palaeoproductivity proxy in an
534 Antarctic polynya environment. The C_{18} and C_{24} compounds yielded the best isotope measurements and show
535 very different $\delta^{13}\text{C}$ trends, suggesting they are being produced by different species in different habitats and/or
536 seasons.

537 Comparison with other proxy data and information from previous studies suggests that the C_{18} compound may
538 be predominantly produced by *P. antarctica*, with $\delta^{13}\text{C}_{18\text{FA}}$ reflecting productivity changes in the marginal ice
539 zone, where it is sensitive to changes in ice cover. In contrast, $\delta^{13}\text{C}_{24\text{FA}}$, which compares well with abundances
540 of the open water diatom *F.s kerguelensis*, may be reflecting summer productivity further offshore, in open
541 waters where it is less sensitive to fast ice changes. We argue that FA $\delta^{13}\text{C}$ can be used as a productivity proxy,
542 but should be used in parallel with other proxies such as diatoms abundances or HBIs. The use of $\delta^{13}\text{C}$ analysis
543 of multiple FA compounds, as opposed to individual compounds or bulk isotope analysis, allows a more
544 detailed insight into the palaeoproductivity dynamics of the region, with the potential to separate productivity
545 trends within different habitats.

546 However, there are clearly uncertainties in interpreting the FA $\delta^{13}\text{C}$, and although we have made parsimonious
547 interpretations, many assumptions have been made here. The producers of the C_{18} and especially the C_{24} FAs is
548 a key source of uncertainty and will require further work to further elucidate. The possibility of inputs of FAs
549 from multiple sources, in particular from organisms further up the food chain, has consequences for their
550 interpretation since this could mean the $\delta^{13}\text{C}$ FA is not fully reflecting just surface water conditions. Other key
551 uncertainties are the magnitude of upwelling of CO_2 at the site in comparison to drawdown by phytoplankton,
552 and the potential role of changes in air-sea CO_2 exchange.

553

554 References

- 555 Anderson, R.F., Ali, S., Bradtmiller, L.I., et al. (2009) Wind-driven upwelling in the Southern Ocean and the
556 deglacial rise in atmospheric CO_2 . *Science (New York, N.Y.)*, 323 (5920): 1443–1448.
557 doi:10.1126/science.1167441.
- 558 Archambeau, A.S., Pierre, C., Poisson, A., et al. (1998) Distributions of oxygen and carbon stable isotopes and
559 CFC-12 in the water masses of the Southern Ocean at 30°E from South Africa to Antarctica: Results of the
560 CIVA1 cruise. *Journal of Marine Systems*, 17 (1–4): 25–38. doi:10.1016/S0924-7963(98)00027-X.
- 561 Arrigo, K.R., van Dijken, G. and Long, M. (2008) Coastal Southern Ocean: A strong anthropogenic CO_2 sink.
562 *Geophysical Research Letters*, 35 (21): 1–6. doi:10.1029/2008GL035624.
- 563 Arrigo, K.R. and van Dijken, G.L. (2003) Phytoplankton dynamics within 37 Antarctic coastal polynya systems.
564 *Journal of Geophysical Research*, 108 (C8): 3271. doi:10.1029/2002JC001739.



- 565 Arrigo, K.R., van Dijken, G.L. and Strong, A.L. (2015) Environmental controls of marine productivity hot spots
566 around Antarctica Kevin. *Journal of Geophysical Research: Oceans*, pp. 2121–2128. doi:10.1002/jgrc.20224.
- 567 Arrigo, K.R., Robinson, D.H., Worthen, D.L., et al. (1999) Community Phytoplankton Structure and the
568 Drawdown of and CO₂ in the Nutrients Southern Ocean. *Science*, 283 (5400): 365–367.
- 569 Ashley, K. E., Bendle, J. A., McKay, R., Etourneau, J., Jimenez-Espejo, F. J., Condrón, A., Albot, A., Crosta,
570 X., Riesselman, C., Seki, O., Massé, G., Gollidge, N. R., Gasson, E., Lowry, D. P., Barrand, N. E., Johnson, K.,
571 Bertler, N., Escutia, C., and Dunbar, R.: Mid-Holocene Antarctic sea-ice increase driven by marine ice sheet
572 retreat, *Clim. Past Discuss.*, <https://doi.org/10.5194/cp-2020-3>, in review, 2020.
- 573 Belt, S.T., Allard, W.G., Rintatalo, J., et al. (2000) Clay and acid catalysed isomerisation and cyclisation
574 reactions of highly branched isoprenoid (HBI) alkenes: Implications for sedimentary reactions and distributions.
575 *Geochimica et Cosmochimica Acta*, 64 (19): 3337–3345. doi:10.1016/S0016-7037(00)00444-0.
- 576 Belt, S.T., Brown, T.A., Smik, L., et al. (2017) Identification of C₂₅ highly branched isoprenoid (HBI) alkenes
577 in diatoms of the genus *Rhizosolenia* in polar and sub-polar marine phytoplankton. *Organic Geochemistry*, 110:
578 65–72. doi:10.1016/j.orggeochem.2017.05.007.
- 579 Belt, S.T. and Müller, J. (2013) The Arctic sea ice biomarker IP 25 : a review of current understanding ,
580 recommendations for future research and applications in palaeo sea ice reconstructions. *Quaternary Science*
581 *Reviews*, 79: 9–25. doi:10.1016/j.quascirev.2012.12.001.
- 582 Belt, S.T., Smik, L., Brown, T.A., et al. (2016) Source identification and distribution reveals the potential of the
583 geochemical Antarctic sea ice proxy IPSO25. *Nature Communications*, 7: 1–10. doi:10.1038/ncomms12655.
- 584 Beucher, C., Tre, P., Hapette, A., et al. (2004) Intense summer Si-recycling in the surface Southern Ocean., 31:
585 0–3. doi:10.1029/2003GL018998.
- 586 Budge, S.M., Wooller, M.J., Springer, A.M., et al. (2008) Tracing carbon flow in an arctic marine food web
587 using fatty acid-stable isotope analysis. *Oecologia*, 157 (1): 117–129. doi:10.1007/s00442-008-1053-7.
- 588 Burke, A. and Robinson, L.F. (2012) The Southern Ocean’s Role in Carbon Exchange During the Last
589 Deglaciation. *Science*, 335: 557–561.
- 590 Cabedo Sanz, P., Smik, L. and Belt, S.T. (2016) On the stability of various highly branched isoprenoid (HBI)
591 lipids in stored sediments and sediment extracts. *Organic Geochemistry*, 97: 74–77.
592 doi:10.1016/j.orggeochem.2016.04.010.
- 593 Campagne, P. (2015) *Étude de la variabilité des conditions océanographiques et climatiques en Antarctique de*
594 *l’Est (Terre Adélie-Georges V) au cours de l’Holocène tardif et de la période instrumentale*. L’Université de
595 Bordeaux.
- 596 Ceccaroni, L., Frank, M., Frignani, M., Langone, L., Ravaioli, M. & Mangini, A. 1998. Late Quaternary
597 fluctuations of biogenic component fluxes on the continental slope of the Ross Sea, Antarctica. *Journal of*
598 *Marine Systems*, 17, 515–525.



- 599 Chiba, S., Hirawake, T., Ushio, S., et al. (2000) An overview of the biological/oceanographic survey by the
600 RTV Umitaka-Maru III off Adelie Land, Antarctica in January-February 1996. *Deep-Sea Research Part II:*
601 *Topical Studies in Oceanography*, 47 (12–13): 2589–2613. doi:10.1016/S0967-0645(00)00037-0.
- 602 Colombo, J.C., Silverberg, N. and Gearing, J.N. (1997) Lipid biogeochemistry in the Laurentian Trough--II.
603 Changes in composition of fatty acids, sterols and aliphatic hydrocarbons during early diagenesis. *Org.*
604 *Geochem.*, 26 (3): 257–274.
- 605 Crosta, X., Crespin, J., Billy, I., et al. (2005) Major factors controlling Holocene d13Corg changes in a seasonal
606 sea-ice environment, Adelie Land, East Antarctica. *Global Biogeochemical Cycles*, 19 (4).
607 doi:10.1029/2004GB002426.
- 608 Crosta, X., Debret, M., Denis, D., et al. (2007) Holocene long- and short-term climate changes off Adelie Land,
609 East Antarctica. *Geochemistry Geophysics Geosystems*, 8 (11): n/a-n/a. doi:10.1029/2007GC001718.
- 610 Crosta X, Shukla S.K., Ther O., Ikehara M., Yamane M., Yokoyama Y. (2020) Last Abundant Appearance
611 Datum of *Hemidiscus karstenii* driven by climate change. *Marine Micropaleontology*,
612 doi:10.1016/j.marmicro.2020.101861.
- 613 Dalsgaard, J., St. John, M., Kattner, G., et al. (2003) Fatty acid trophic markers in the pelagic marine
614 environment. *Advances in Marine Biology*. 46 pp. 225–340. doi:10.1016/S0065-2881(03)46005-7.
- 615 DiTullio, G.R., Grebmeier, J.M., Arrigo, K.R., et al. (2000) Rapid and early export of Phaeocystis antarctica
616 blooms in the Ross Sea, Antarctica. *Nature*, 404 (6778): 595–598. doi:10.1038/35007061.
- 617 Escutia, C., Brinkhuis, H., Klaus, A., et al. (2011) *Expedition 318 summary*.
618 doi:10.2204/iodp.proc.318.101.2011.
- 619 Farquhar, G.D., O’Leary, M.H. and Berry, J.A. (1982) On the Relationship between Carbon Isotope
620 Discrimination and the Intercellular Carbon dioxide Concentration in Leaves. *Australian Journal of Plant*
621 *Physiology*, 9: 121–137.
- 622 Fischer, G., Schneider, R., Müller, P.J., et al. (1997) Anthropogenic CO₂ in Southern Ocean surface waters:
623 Evidence from stable organic carbon isotopes. *Terra Nova*, 9 (4): 153–157. doi:10.1046/j.1365-3121.1997.d01-
624 29.x.
- 625 Francey, R.J., Allison, C.E., Etheridge, D.M., et al. (1999) A 1000-year high precision record of δ¹³C in
626 atmospheric CO₂. *Tellus, Series B: Chemical and Physical Meteorology*, 51 (2): 170–193.
- 627 Frignani, M., Giglio, F., Langone, L., Ravaioli, M. & Mangini, A. 1998. Late Pleistocene- Holocene
628 sedimentary fluxes of organic carbon and biogenic silica in the northwestern Ross Sea, Antarctica. *Annals of*
629 *Glaciology*, 27, 697–703.
- 630
- 631 Gibson, J.A.E., Trull, T., Nichols, P.D., et al. (1999) Sedimentation of ¹³C-rich organic matter from Antarctic
632 sea-ice algae: A potential indicator of past sea-ice extent. *Geology*, 27 (4): 331–334. doi:10.1130/0091-
633 7613(1999)027<0331:SOCROM>2.3.CO;2.



- 634 Gilchrist, H. (2018) *A high-resolution record of sea ice, glacial and biological dynamics from an Antarctic*
635 *coast environment*. University of Birmingham.
- 636 Haddad, R.I., Martens, C.S. and Farrington, J.W. (1992) Quantifying early diagenesis of fatty acids in a rapidly
637 accumulating coastal marine sediment. *Organic Geochemistry*, 19 (1–3): 205–216. doi:10.1016/0146-
638 6380(92)90037-X.
- 639 Henley, S.F., Annett, A.L., Ganeshram, R.S., et al. (2012) Factors influencing the stable carbon isotopic
640 composition of suspended and sinking organic matter in the coastal Antarctic sea ice environment.
641 *Biogeosciences*, 9 (3): 1137–1157. doi:10.5194/bg-9-1137-2012.
- 642 Johns, L. et al. (1999) ‘Identification of a C25 highly branched isoprenoid (HBI) diene in Antarctic sediments,
643 Antarctic sea-ice diatoms and cultured diatoms’, *Organic Geochemistry*, 30(11), pp. 1471–1475. doi:
644 10.1016/S0146-6380(99)00112-6.
- 645 Keeling, C.D., Piper, S.C., Bacastow, R.B., et al. (2005) “Atmospheric CO₂ and ¹³CO₂ Exchange with the
646 Terrestrial Biosphere and Oceans from 1978 to 2000: Observations and Carbon Cycle Implications.” In A
647 History of Atmospheric CO₂ and Its Effects on Plants, Animals, and Ecosystems. doi:10.1007/0-387-27048-
648 5_5.
- 649 Kopczyńska, E.E., Goeyens, L., Semeneh, M., et al. (1995) Phytoplankton Composition and Cell Carbon
650 Distribution in Prydz Bay, Antarctica - Relation To Organic Particulate Matter and Its Delta-C-13 Values.
651 *Journal of Plankton Research*, 17 (4): 685–707. doi:10.1093/plankt/17.4.685.
- 652 Leblond, J.D. and Chapman, P.J. (2000) LIPID CLASS DISTRIBUTION OF HIGHLY UNSATURATED
653 LONG CHAIN FATTY ACIDS IN MARINE DINOFLAGELLATES. *Journal of Phycology*, 36: 1103–1108.
- 654 MacFarling Meure, C., Etheridge, D., Trudinger, C., et al. (2006) Law Dome CO₂, CH₄ and N₂O ice core
655 records extended to 2000 years BP. *Geophysical Research Letters*, 33 (14): 1–4. doi:10.1029/2006GL026152.
- 656 Mackensen, A. (2001) Oxygen and carbon stable isotope tracers of Weddell sea water masses: New data and
657 some paleoceanographic implications. *Deep-Sea Research Part I: Oceanographic Research Papers*, 48 (6):
658 1401–1422. doi:10.1016/S0967-0637(00)00093-5.
- 659 Massé, G., Belt, S.T., Crosta, X., et al. (2011) Highly branched isoprenoids as proxies for variable sea ice
660 conditions in the Southern Ocean. *Antarctic Science*, 23 (5): 487–498. doi:10.1017/S0954102011000381.
- 661 Matsuda, H. (1978) Early diagenesis of fatty acids in lacustrine sediments-III. Changes in fatty acid composition
662 in the sediments from a brackish water lake. *Geochimica et Cosmochimica Acta*, 42: 1027–1034.
- 663 Matsuda, H. and Koyama, T. (1977) Early diagenesis of fatty acids in lacustrine sediments-I. Identification and
664 distribution of fatty acids in recent sediment from a freshwater lake. *Geochimica et Cosmochimica Acta*, 41 (6):
665 777–783. doi:10.1016/0016-7037(77)90048-5.
- 666 Moisan, T.A. and Mitchell, B.G. (1999) Photophysiological acclimation of *Phaeocystis antarctica* Karsten under
667 light limitation. *Limnology and Oceanography*, 44 (2): 247–258. doi:10.4319/lo.1999.44.2.0247.



- 668 Pancost, R.D. and Boot, C.S. (2004) The palaeoclimatic utility of terrestrial biomarkers in marine sediments.
669 *Marine Chemistry*, 92 (1–4 SPEC. ISS.): 239–261. doi:10.1016/j.marchem.2004.06.029.
- 670 Poulton, A.J., Mark Moore, C., Seeyave, S., et al. (2007) Phytoplankton community composition around the
671 Crozet Plateau, with emphasis on diatoms and Phaeocystis. *Deep-Sea Research Part II: Topical Studies in*
672 *Oceanography*, 54 (18–20): 2085–2105. doi:10.1016/j.dsr2.2007.06.005.
- 673 Rau, G.H., Takahashi, T. and Des Marais, D.J. (1989) Latitudinal variations in plankton $\delta^{13}\text{C}$: Implications for
674 CO₂ and productivity in past oceans. *Nature*, 341 (6242): 516–518.
- 675 Riaux-gobin, C., Dieckmann, G.S., Poulin, M., et al. (2013) *Environmental conditions , particle flux and*
676 *sympagic microalgal succession in spring before the sea-ice break-up in Adélie Land , East Antarctica*
677 *Environmental conditions , particle flux and sympagic microalgal succession in spring before t.,*
678 (May 2014): 0–25. doi:10.3402/polar.v32i0.19675.
- 679 Riaux-Gobin, C., Dieckmann, G.S., Poulin, M., et al. (2013) Environmental conditions, particle flux and
680 sympagic microalgal succession in spring before the sea-ice break-up in Adélie Land, East Antarctica. *Polar*
681 *Research*, 32 (SUPPL.): 0–25. doi:10.3402/polar.v32i0.19675.
- 682 Riaux-Gobin, C., Poulin, M., Dieckmann, G., et al. (2011) Spring phytoplankton onset after the ice break-up and
683 sea-ice signature (Adélie Land, East Antarctica). *Polar Research*, 30 (SUPPL.1).
684 doi:10.3402/polar.v30i0.5910.
- 685 Roden, N.P., Shadwick, E.H., Tilbrook, B., et al. (2013) Annual cycle of carbonate chemistry and decadal
686 change in coastal Prydz Bay, East Antarctica. *Marine Chemistry*, 155: 135–147.
687 doi:10.1016/j.marchem.2013.06.006.
- 688 Salminen, T.A., Eklund, D.M., Joly, V., et al. (2018) Deciphering the evolution and development of the cuticle
689 by studying lipid transfer proteins in mosses and liverworts. *Plants*, 7 (1). doi:10.3390/plants7010006.
- 690 Sambrotto, R.N., Matsuda, A., Vaillancourt, R., et al. (2003) Summer plankton production and nutrient
691 consumption patterns in the Mertz Glacier Region of East Antarctica. *Deep-Sea Research Part II: Topical*
692 *Studies in Oceanography*, 50 (8–9): 1393–1414. doi:10.1016/S0967-0645(03)00076-6.
- 693 Shadwick, E.H., Tilbrook, B. and Williams, G.D. (2014) Carbonate chemistry in the Mertz Polynya (East
694 Antarctica): Biological and physical modification of dense water outflows and the export of anthropogenic CO₂.
695 *Journal of Geophysical Research: Oceans*, 119 (1): 1–14. doi:10.1002/2013JC009286.
- 696 Shevenell, A.E. and Kennett, J.P. (2002) *Antarctic Holocene climate change : A benthic foraminiferal stable*
697 *isotope record from Palmer Deep.*, 17 (2).
- 698 Sigman, D. and Boyle, E. (2000) Glacial/interglacial variations in atmospheric carbon dioxide. *Nature*, 407
699 (6806): 859–869.
- 700 Sinninghe Damsté, J.S., Rijpstra, W.I.C., Coolen, M.J.L., et al. (2007) Rapid sulfuration of highly branched
701 isoprenoid (HBI) alkenes in sulfidic Holocene sediments from Ellis Fjord, Antarctica. *Organic Geochemistry*,
702 38 (1): 128–139. doi:10.1016/j.orggeochem.2006.08.003.



- 703 Skerratt, J.H., Davidson, A.D., Nichols, P.D., et al. (1998) Effect of UV-B on lipid content of three antarctic
704 marine phytoplankton. *Phytochemistry*, 49 (4): 999–1007. doi:10.1016/S0031-9422(97)01068-6.
- 705 Smik, L., Belt, S.T., Lieser, J.L., et al. (2016) Distributions of highly branched isoprenoid alkenes and other
706 algal lipids in surface waters from East Antarctica: Further insights for biomarker-based paleo sea-ice
707 reconstruction. *Organic Geochemistry*, 95: 71–80. doi:10.1016/j.orggeochem.2016.02.011.
- 708 Sun, M.Y., Zou, L., Dai, J., et al. (2004) Molecular carbon isotopic fractionation of algal lipids during
709 decomposition in natural oxic and anoxic seawaters. *Organic Geochemistry*, 35 (8): 895–908.
710 doi:10.1016/j.orggeochem.2004.04.001.
- 711 Sweeney, C. (2003) “The annual cycle of surface water CO₂ And O₂ in the Ross Sea: A model for gas
712 exchange on the continental shelves of Antarctica.” *In Antarctic Research Series Vol 78*. doi:10.1029/078ars19.
- 713 Takahashi, T., Sutherland, S.C., Wanninkhof, R., et al. (2009) Climatological mean and decadal change in
714 surface ocean pCO₂, and net sea-air CO₂ flux over the global oceans. *Deep-Sea Research Part II: Topical
715 Studies in Oceanography*, 56 (8–10): 554–577. doi:10.1016/j.dsr2.2008.12.009.
- 716 Tortell, P.D., Guéguen, C., Long, M.C., et al. (2011) Spatial variability and temporal dynamics of surface water
717 pCO₂, δO₂/Ar and dimethylsulfide in the Ross Sea, Antarctica. *Deep-Sea Research Part I: Oceanographic
718 Research Papers*, 58 (3): 241–259. doi:10.1016/j.dsr.2010.12.006.
- 719 Tréguer, P., Bowler, C., Moriceau, B., et al. (2017) Influence of diatom diversity on the ocean biological carbon
720 pump. *Nature Geoscience*. doi:10.1038/s41561-017-0028-x.
- 721 Vaillancourt, R.D., Sambrotto, R.N., Green, S., et al. (2003) Phytoplankton biomass and photosynthetic
722 competency in the summertime Mertz Glacier region of East Antarctica. *Deep-Sea Research Part II: Topical
723 Studies in Oceanography*, 50 (8–9): 1415–1440. doi:10.1016/S0967-0645(03)00077-8.
- 724 Villinski, J.C., Hayes, J.M., Brassell, S.C., et al. (2008) Sedimentary sterols as biogeochemical indicators in the
725 Southern Ocean. *Organic Geochemistry*, 39 (5): 567–588. doi:10.1016/j.orggeochem.2008.01.009.
- 726 Wakeham, S.G., Lee, C., Farrington, J.W., et al. (1984) Biogeochemistry of particulate organic matter in the
727 oceans: results from sediment trap experiments. *Deep Sea Research Part A, Oceanographic Research Papers*,
728 31 (5): 509–528. doi:10.1016/0198-0149(84)90099-2.
- 729 Williams, G.D. and Bindoff, N.L. (2003) Wintertime oceanography of the Adélie Depression. *Deep-Sea
730 Research Part II: Topical Studies in Oceanography*, 50 (8–9): 1373–1392. doi:10.1016/S0967-0645(03)00074-
731 2.
- 732 Wilson, D.L., Smith, W.O. and Nelson, David, M. (1986) *Phytoplankton bloom dynamics of the western Ross
733 Sea ice edge - I. Primary productivity and species-specific production.*, 33 (10): 1375–1387.
- 734 Wong, W.W. and Sackett, W.M. (1978) Fractionation of stable carbon isotopes by marine phytoplankton.
735 *Geochimica et Cosmochimica Acta*, 42 (12): 1809–1815. doi:10.1016/0016-7037(78)90236-3.
- 736 Zhang, R., Zheng, M., Chen, M., et al. (2014) An isotopic perspective on the correlation of surface ocean carbon



737 dynamics and sea ice melting in Prydz Bay (Antarctica) during austral summer. *Deep-Sea Research Part I:*
 738 *Oceanographic Research Papers*, 83: 24–33. doi:10.1016/j.dsr.2013.08.006.

739

740

741

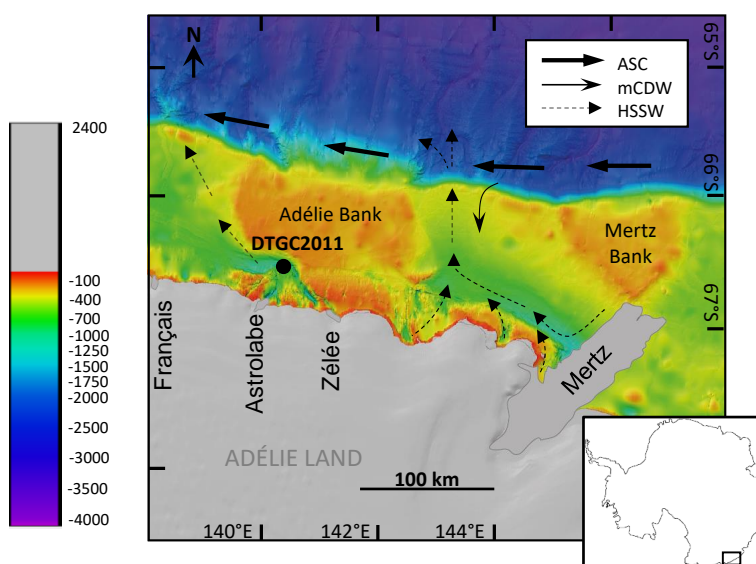


Figure 1: Location of Site DTGC2011 on bathymetric map of the Adélie Land region (modified from Beaman et al., 2011), indicating positions of the main glaciers (prior to Mertz Glacier Tongue collapse in 2010) and pathways of the main water masses affecting the region: Antarctic Slope Current (ASC), Modified Circumpolar Deep Water (mCDW) and High Shelf Salinity Water (HSSW) (Williams and Bindoff, 2003).

742

743

744

745

746

747

748

749

750

751

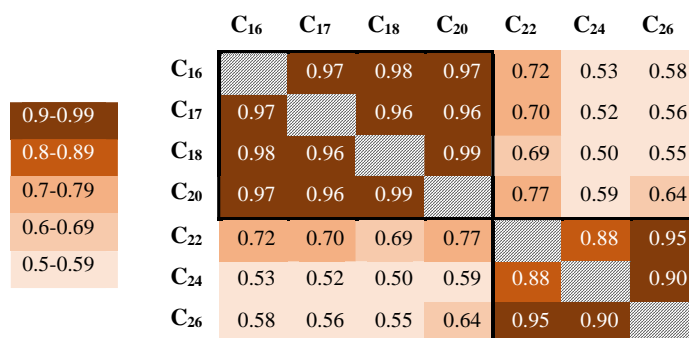


Figure 2: R² values for fatty acid concentrations throughout core DTGC2011. Values are colour coded according to the key on the left. Black border denotes correlations within each group.

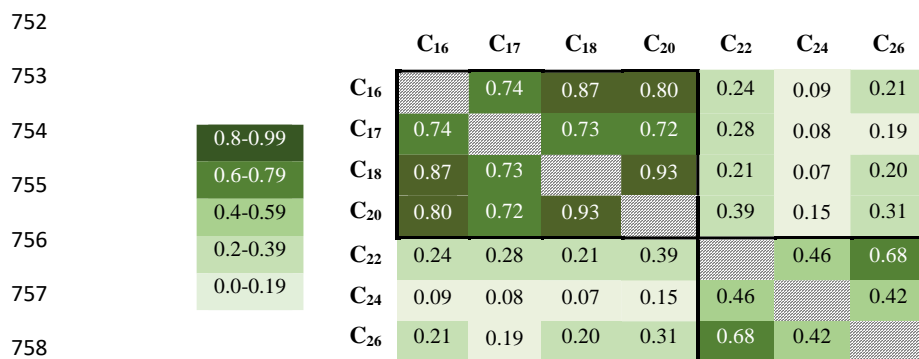


Figure 3: R² values for fatty acid concentrations in core DTGC2011 below 25 cm only. Values are colour coded according to the key on the left. Black border denotes correlations within each group.

759
 760
 761
 762
 763
 764
 765
 766



767

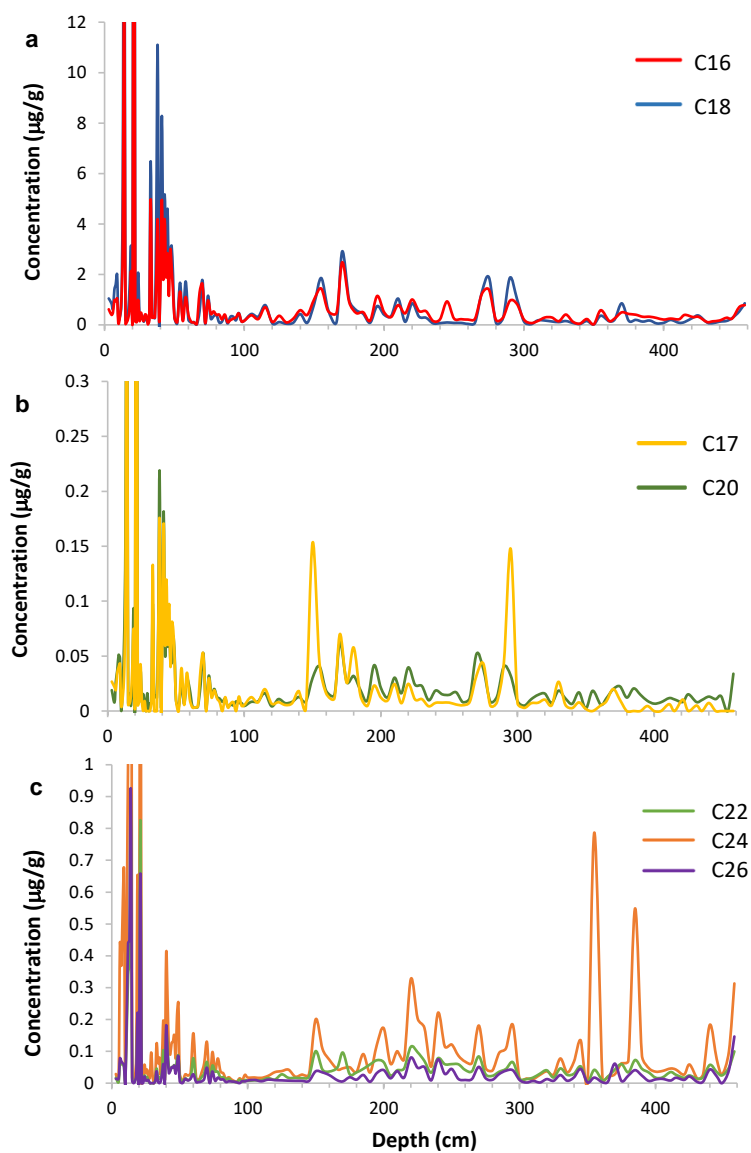


Figure 4: Fatty acid concentrations ($\mu\text{g/g}$ of dry sediment) with depth from core DTGC2011
a) C₁₆ and C₁₈ fatty acids b) C₁₇ and C₂₀ fatty acids c) C₂₂, C₂₄ and C₂₆ fatty acids.

768

769

770



771

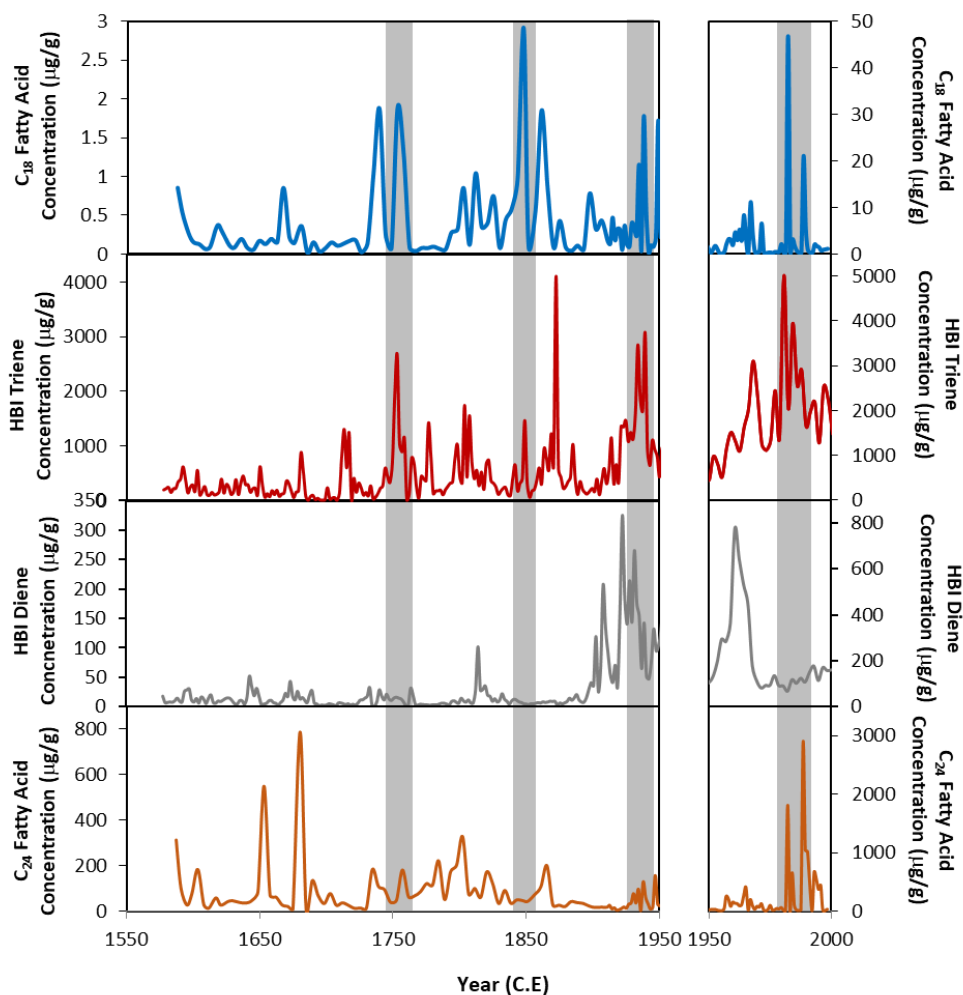


Figure 5: Concentrations of the C_{18} fatty acid (blue), the HBI triene (red), HBI diene (grey) (Campagne, 2015), C_{24} fatty acid (orange) from core DTGC2011. The left-hand panels show 1550 to 1950 C.E. and the right hand panels show 1950 to 2000 C.E., plotted on different y-axes due to the elevated concentrations in the top part of the core. Grey vertical bands highlight coincident peaks in C_{18} fatty acid and HBI triene records.

772

773

774

775

776

777



778

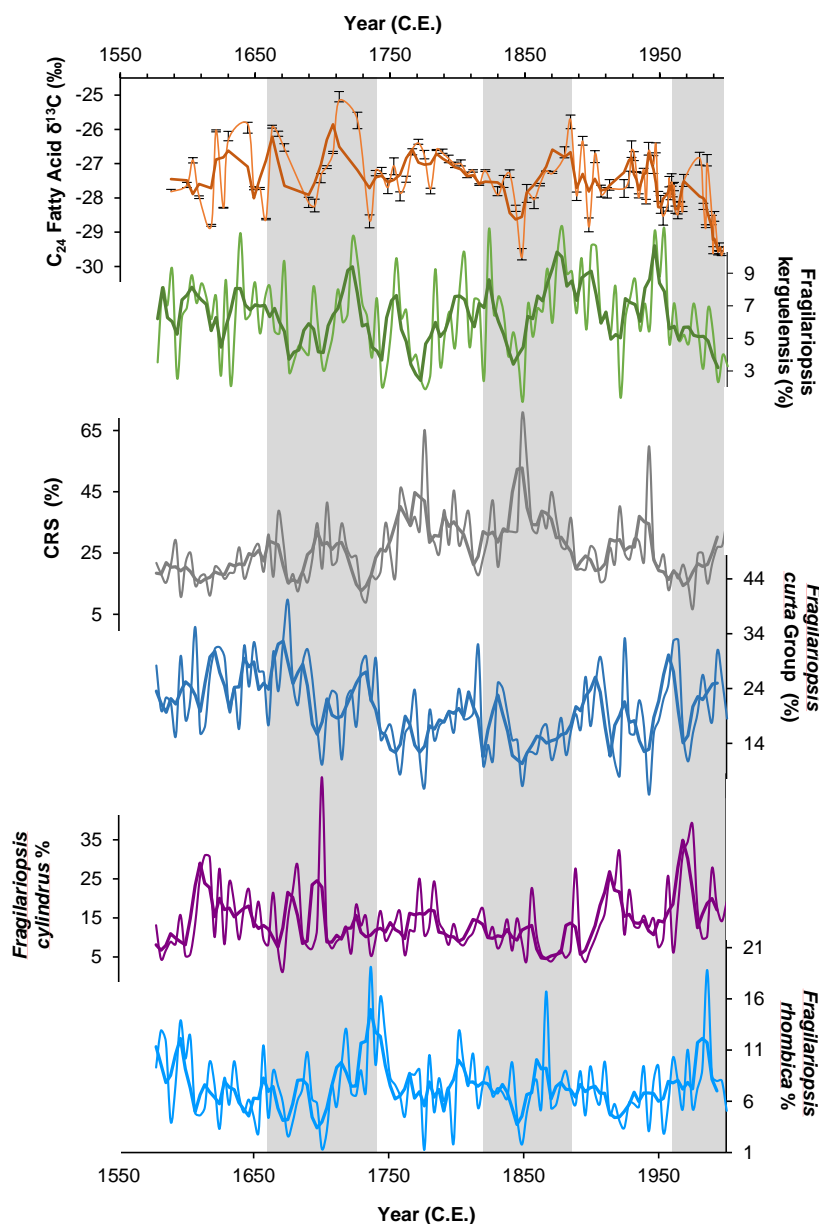


Figure 6: $\delta^{13}C$ values of the C_{24} fatty acid (orange) and relative abundances (%) of the open water diatom *Fragilariopsis kerguelensis* (green). Also shown are relative abundances of the four most abundant diatom groups in DTGC2011. *Chaetoceros* resting spores (CRS; grey line), *Fragilariopsis curta* group (dark blue line), *Fragilariopsis cylindrus* (purple line) and *Fragilariopsis rhombica* (light blue line). Thick line represents 3-point moving average for each. Grey vertical bands highlight periods where C_{24} fatty acid $\delta^{13}C$ is in phase with *F. kerguelensis*.



779

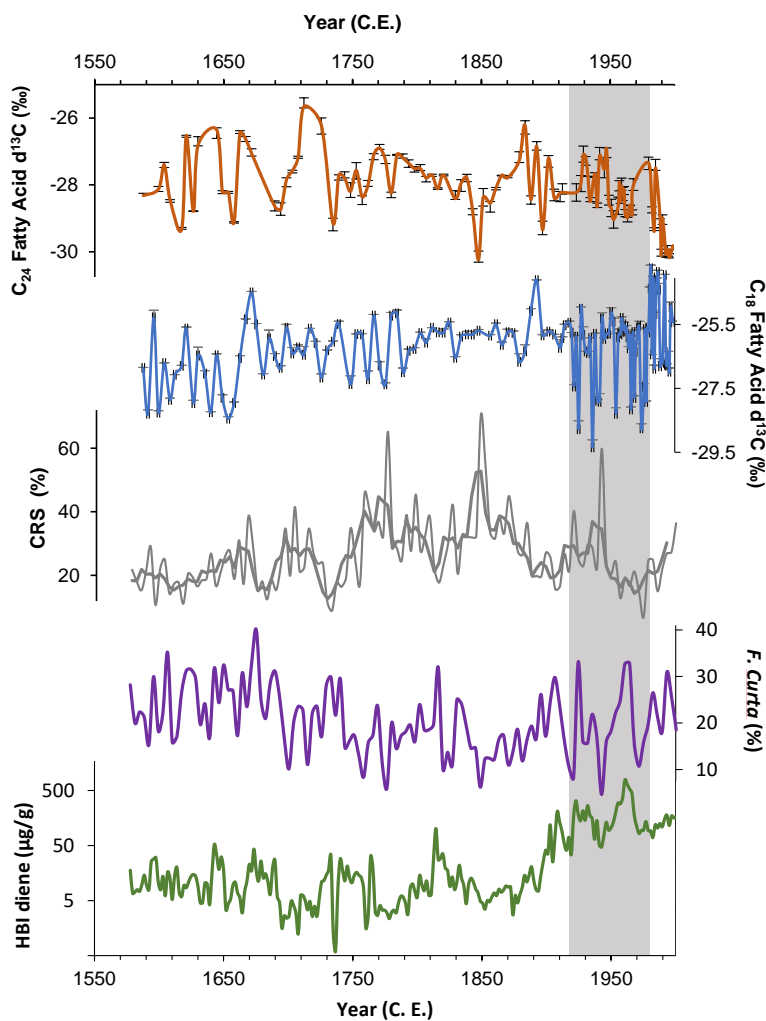


Figure 7: $\delta^{13}\text{C}$ of the C_{24} (orange) and C_{18} (blue) fatty acid, HBI diene concentrations (green; plotted on a log scale) and relative abundances of *Fragilariopsis curta* plus *Fragilariopsis cylindrus* (purple). Latter two records reflect sea ice concentrations. Grey vertical band highlights period where low C_{18} $\delta^{13}\text{C}$ overlaps with elevated HBI diene concentrations.

780

781